# Bactericidal Activity of Partially Oxidized Nanodiamonds

**Julia Wehling,[†] Ralf Dringen,[‡] Richard N. Zare,[§] Michael Maas,[†,*] and Kurosch Rezwan[†]**

[†]Advanced Ceramics, University of Bremen, Am Biologischen Garten 2, 28359 Bremen, Germany, [‡]Centre for Biomolecular Interactions Bremen, Faculty 2 (Biology/Chemistry) and Centre for Environmental Research and Sustainable Technology, University of Bremen, Leobener Straße NW2, 28359 Bremen, Germany, and [§]Department of Chemistry, Stanford University, Stanford, California 94305-5080, United States

**ABSTRACT** Nanodiamonds are a class of carbon-based nanoparticles that are rapidly gaining attention, particularly for biomedical applications, *i.e.*, as drug carriers, for bioimaging, or as implant coatings. Nanodiamonds have generally been considered biocompatible with a broad variety of eukaryotic cells. We show that, depending on their surface composition, nanodiamonds kill Gram-positive and -negative bacteria rapidly and efficiently. We investigated six different types of nanodiamonds exhibiting diverse oxygen-containing surface groups that were created using standard pretreatment methods for forming nanodiamond dispersions. Our experiments suggest that the antibacterial activity of nanodiamond is linked to the presence of partially oxidized and negatively charged surfaces, specifically those containing acid anhydride groups. Furthermore, proteins were found to control the bactericidal properties of nanodiamonds by covering these surface groups, which explains the previously reported biocompatibility of nanodiamonds. Our findings describe the discovery of an exciting property of partially oxidized nanodiamonds as a potent antibacterial agent.

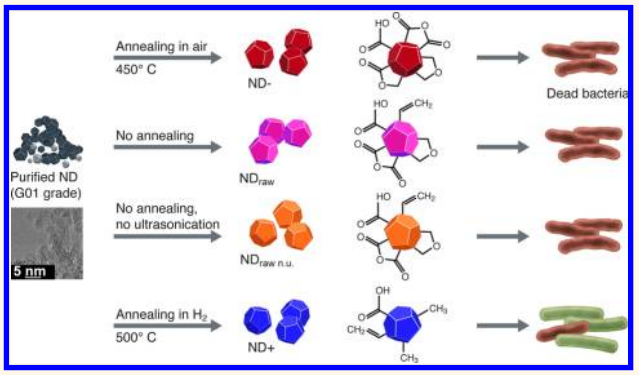


**KEYWORDS:** nanodiamond · antibacterial · anhydride · *E. coli* · *B. subtilis*

The application of nanoparticles in the biomedical field naturally results in the increased scrutiny of the possible toxicity of nanoparticles. While adverse effects could be clearly demonstrated in only a few cases,[1−5] great controversy usually accompanies the establishment of a new nanomaterial. Nanodiamonds (NDs) are among the most promising new materials for biomedical applications. We elucidated the effect of NDs on bacterial viability in an extensive study using six different types of NDs that were derived from slightly different standard pretreatments. After analyzing the material properties of the diverse NDs, we performed antibacterial tests on Gram-negative *Escherichia coli* and Gram-positive *Bacillus subtilis*. Our experiments clearly showed extraordinary antibacterial activity for some of the ND species.

In the past few years, progress in purifying and disaggregating has enabled the dispersion of discrete NDs in physiological solutions.[6] With this development, the usage of this $sp^3$-hybridized carbon nanomaterial, which has been known for more than 60 years,[7] has markedly increased. Small NDs in the range of 2−10 nm are produced by the detonation of carbon-containing explosives under an oxygen-deficient atmosphere. Detonation NDs are composed of an $sp^3$-carbon diamond core and a graphitized outer layer containing $sp^2$-hybridized carbon that is partially oxidized with a variety of oxygen species[8] and contains a negative electrostatic potential on most facets in the presence of inorganic salts.[9] The graphitized outer layer enables functionalization with different surface groups, which, in turn, leads to a variety of unique surface functionalities dependent on pretreatment and processing. Owing to their exceptional characteristics such as fluorescence,[10,11] chemical inertness, and the potential for surface functionalization,[12] NDs can be applied in a variety of biomedical applications. These include bioimaging,[10] drug delivery,[13,14] implant coating,[14] and reinforcement.[13] So far, literature data indicate that NDs are nontoxic for eukaryotic cells,[15] but investigations on the biocompatibility

* Address correspondence to michael.maas@uni-bremen.de.

Received for review April 23, 2014 and accepted May 26, 2014.

**Published online May 26, 2014**
**10.1021/nn502230m**

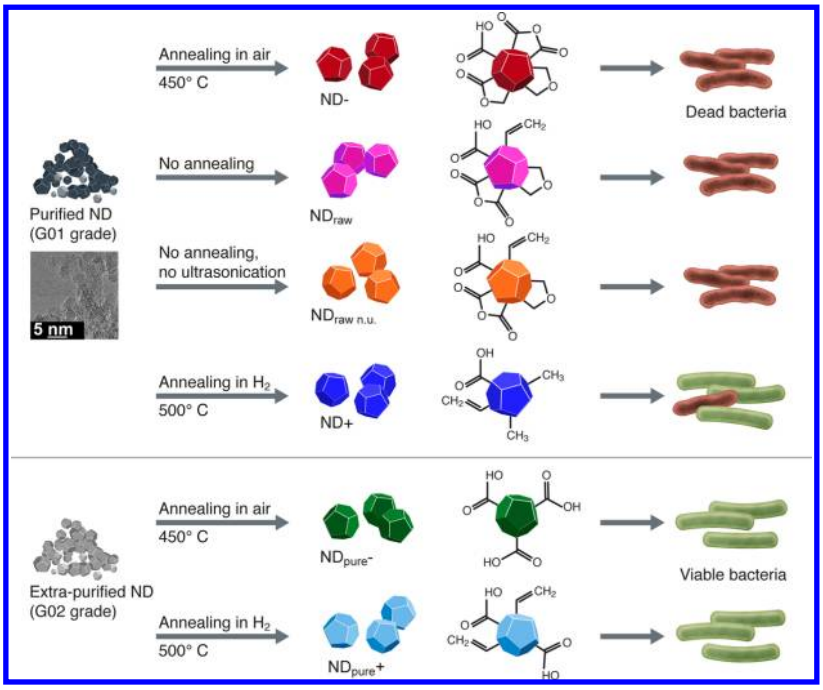


**Figure 1. Grades and pretreatments of NDs. Nanodiamond powder of two different purity grades was annealed in air to generate negatively charged NDs (ND−, $ND_{pure}$−) and in an $H_2$ atmosphere to obtain positively charged NDs (ND+, $ND_{pure}$+). Raw powder of G01 grade without former pretreatments was diluted in water and dispersed with ($ND_{raw}$) or without ultrasonication ($ND_{raw\ n.u.}$). (a) Negatively charged ND− and $ND_{raw}$/$ND_{raw\ n.u.}$ were shown to exhibit strong antibacterial properties under aqeuous conditions, while ND+ caused bacterial death only at high ND concentrations. (b) $ND_{pure}$, independent of their charge, did not show any bactericidal effects (b).**

of NDs with small organisms and prokaryotes are rare.[16−18]

## RESULTS AND DISCUSSION

Our study started with standard pretreatment procedures according to Hees *et al.*[19] to generate differently charged NDs. For this, purified ND of G01 grade (ND) and ND of G02 grade ($ND_{pure}$), which were further purified by the manufacturer using oxygenating methods, were annealed under two different conditions, resulting in negatively and positively charged NDs (Figure 1). Annealing in air gave rise to negatively charged ND− and $ND_{pure}$−, and annealing in an $H_2$ atmosphere led to positively charged ND+ and $ND_{pure}$+. After annealing, the different ND types were disaggregated using high-energy ultrasound. These pretreatments enabled the stable dispersion of the NDs in aqueous suspensions. Furthermore, raw powder of G01 grade without previous annealing was diluted in water with ($ND_{raw}$) or without ultrasonication ($ND_{raw\ n.u.}$). Dispersions of both were not stable, and ND tended to agglomerate and sediment soon after mixing due to the missing annealing step (data not shown).

Zeta potential measurements revealed negative charges for ND− and $ND_{pure}$− with values of −44 and −77 mV, respectively, while the positively charged particles had values of +63 mV (ND+) and +80 mV ($ND_{pure}$+) (Table 1). The zeta potential of $ND_{raw}$ and $ND_{raw\ n.u.}$ could not be determined due to polydispersity. Particle sizes measured by dynamic light scattering (DLS) were around 60 nm weighted by intensity and around 4 nm weighted by numbers (data not shown). The surface chemistry of all particles was analyzed using Fourier transform infrared spectroscopy (FTIR). While the surfaces of $ND_{pure}$ contained only carboxyl groups, the surfaces of ND−, ND+, and $ND_{raw}$/$ND_{raw\ n.u.}$ were only partially oxidized and exhibited a variety of reactive oxygen groups, especially acid anhydrides (Figure 2).

With these different types of NDs, it was possible to design a thorough study to elucidate antibacterial properties of NDs. Next to the surface functionalities that were generated by the pretreatment methods, impurities of the ND samples were analyzed in detail to exclude possible side-effects.

To test the bactericidal properties of ND, *E. coli* and *B. subtilis* were used as model organisms. These bacteria were incubated with NDs for 15 min in a weak hypotonic salt buffer at neutral pH in the absence of proteins and low-molecular-weight substances as described in the Methods section. An adenosine triphosphate (ATP)-dependent enzyme that gives rise to luminescence was used to determine bacterial ATP levels (Bac Titer-Glo). The ATP levels serve as a marker for vital bacterial metabolism; ATP levels directly correlate to the number of living cells. As controls, luminescence counts of samples treated

**TABLE 1. Pretreatments and Zeta Potentials of the Different Types of ND ($d \approx 4$ nm)[a]**

| | Annealing | Zeta potential (mV) |
|---|---|---|
| ND- | Air atmosphere, 5h 450°C | -44 ± 2 |
| $ND_{raw}$ | No annealing | Not determined due to polydispersity |
| $ND_{raw}$ n.u. | No annealing | Not determined due to polydispersity |
| ND+ | $H_2$ atmosphere, 4.5h 500°C | +63 ± 2 |
| $ND_{pure}$- | Air atmosphere, 5h 450°C | -77 ± 2 |
| $ND_{pure}$+ | $H_2$ atmosphere, 4.5h 500°C | +80 ± 2 |

[a] Sizes for $ND_{raw}$ and $ND_{raw\ n.u.}$ were not measured due to polydispersity.

without NDs under otherwise identical conditions were set as 100% bacterial viability. In addition, we analyzed the ability of the bacterial cells to grow and form colonies as a second indicator for bacterial viability and determined the number of colony-forming units (CFU).

Our results showed that already after 15 min contact times with ND− and $ND_{raw}$/$ND_{raw\ n.u.}$, the vitality of *E. coli* was almost completely compromised. While concentrations of 500 and 50 mg/L reduced bacterial ATP levels to less than 10% of the values found for untreated *E. coli* cells (Figure 3a), bacterial vitality was also strongly decreased in the presence of ND− and $ND_{raw}$ even at a concentration of 5 mg/L. The antibacterial effect of positively charged ND+ was less powerful. Although a high concentration of 500 mg/L ND+ reduced ATP levels by around 80%, lower ND concentrations did not affect bacterial viability. $ND_{pure}$, whether negatively or positively charged, showed no reduced viability for *E. coli*, even when applied at a high concentration of 500 mg/L (Figure 3a). Almost identical results to those observed for *E. coli* on the antibacterial activity of NDs were found for the Gram-positive bacterium *B. subtilis* (Figure 3b).

Plating ND-treated bacteria and counting CFU for *E. coli* and *B. subtilis* (Figure 3c) confirmed results obtained for the acute effects of NDs on bacterial viability determined by ATP measurements (Figure 3a,b). Results from both types of bacterial viability assays suggest that ND− and $ND_{raw}$/$ND_{raw\ n.u.}$ are highly potent antibacterial materials that rapidly compromise bacterial survival of Gram-positive and -negative bacteria.

To investigate whether NDs are taken up into bacterial cells and/or attach to cellular structures, we incubated *E. coli* with a sublethal ND concentration (0.5 mg/L) and analyzed the localization of NDs in bacteria by transmission electron microscopy (TEM). TEM analysis revealed that ND− had been incorporated by *E. coli*, since we found distinct ND− agglomerates inside the cells (Figure 4a). Cells were deformed in the presence of ND−, showing an irregular shape (Figure 4a,b), which might indicate stress to the bacteria even at sublethal ND− concentrations. Positively charged ND+ seemed mainly to attach to the bacterial cell surface, which can be explained by electrostatic interactions with the negatively charged cell walls.[20] Although ND+ was not found inside the cells, parts of the cellular shapes seemed to be irregular (Figure 4c,d). Similar to ND−, we found $ND_{pure}$− agglomerates inside the cells (Figure 4e). However, concurrent with our results from the viability tests, $ND_{pure}$− did not alter the bacterial shape (Figure 4e,f) since the cell morphology was comparable to the ND− free controls (Figure 4g,h).

Neither the quantification of bacterial ATP levels, CFU determination, nor TEM analysis showed any antibacterial potential of $ND_{pure}$. We first surmised that metal impurities in the slightly less pure ND (grade G01) might cause the bactericidal activity. According to the manufacturer's data (www.plasmachem.com), purified NDs of grade G01 contain controlled admixtures of less than 0.3 wt % Fe and less than 0.01 wt % Cu, Zn, Mn, Si, Cr, Ca, and Ti, derived from the production process, while extrapurified nanodiamonds of grade G02 include less than 0.05 wt % Fe and other metals that do not exceed 0.01 wt %.

Copper and zinc impurities of our ND samples were determined by a complete acidic digestion, which we performed for the different ND types.[21] Concentrations were in the range of 3 $\mu$M for the highest dilution of ND dispersions (500 mg/L) (Supplementary Table 1), and a control experiment showed that copper(II) sulfate did not reduce bacterial ATP levels at concentrations corresponding to the concentrations found in ND dispersions (Supplementary Figure 1). Zinc impurities did not differ between the investigated ND types (Supplementary Table 1).

To exclude the possibility that other soluble, low molecular weight substances caused bacterial death, we dialyzed ND against water and tested the effect of particle-free dialysates on bacteria. Dialysates were diluted 1:10. Nevertheless, neither dialysates that correlate

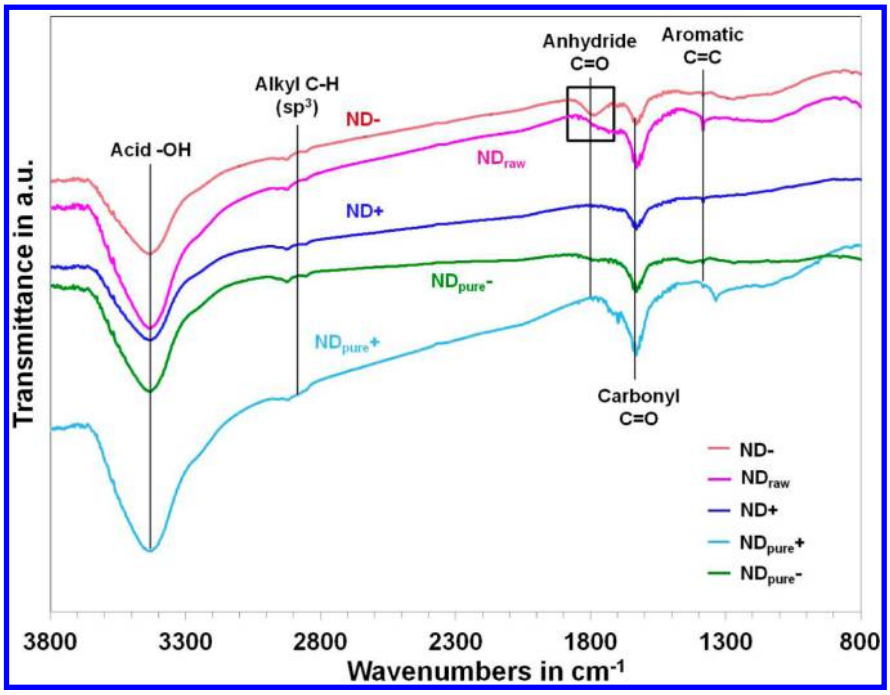


**Figure 2. FTIR spectra of the different ND types. All ND types contain different oyxgen groups on their surface. The absorption band at around 1850−1750 $cm^{-1}$ is attributed to acid anhydride groups, which are present only on the antibacterial types ND− and $ND_{raw}$.**

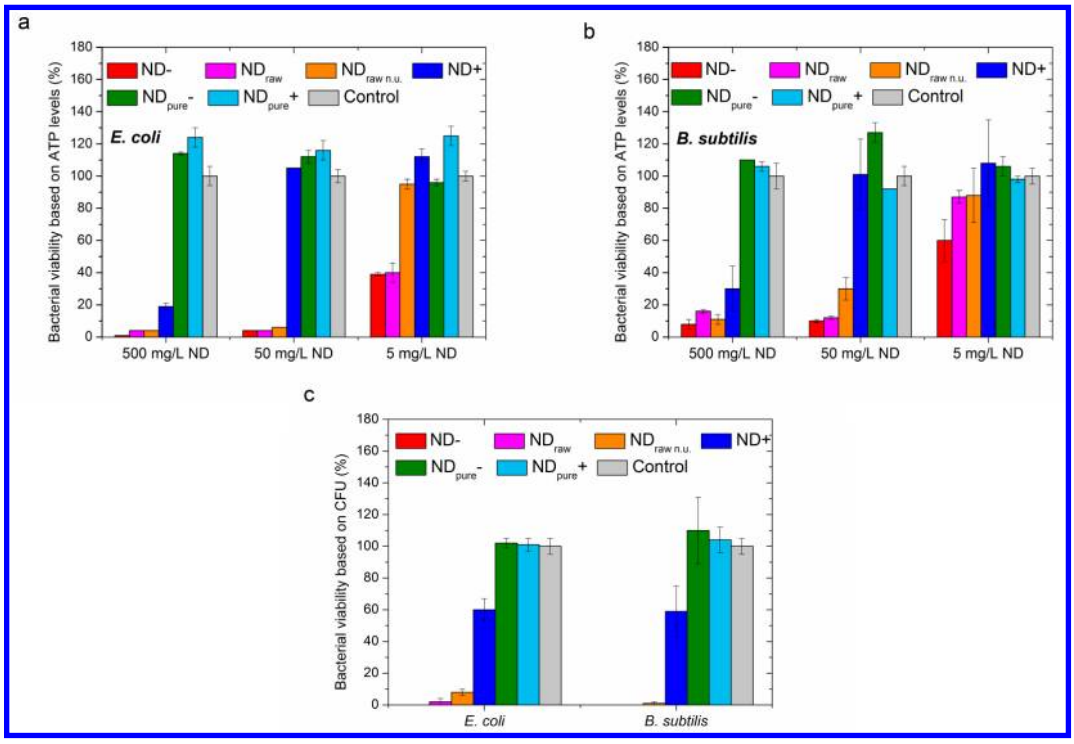


**Figure 3. Antibacterial activity of NDs on *E. coli* and *B. subtilis*. (a, b) Negatively charged ND− and $ND_{raw}$/$ND_{raw\ n.u.}$ strongly decreased bacterial viability measured by ATP levels in 15 min, while positively charged ND+ decrease ATP levels only at the highest ND concentrations for Gram-negative *E. coli* (a) and Gram-positive *B. subtilis* (b). Pure NDs generally do not affect bacterial viabilty (a, b). After incubation with 500 mg/L NDs, the determination of colony-forming units for *E. coli* and *B. subtilis* (c) led to similar trends to the measurement of ATP, indicating that ND− and $ND_{raw}$/$ND_{raw\ n.u.}$ are very effective at inhibiting bacterial growth, while positively charged ND+ are less bactericidal. Again, $ND_{pure}$ does not affect bacterial survival (c).**

to 50 mg/L ND dispersions nor to 5 mg/L dispersions affected bacterial viability, as indicated by unaltered ATP levels and numbers of CFU in comparison to the water controls (Supplementary Figure 2). Therefore, we exclude that toxic low-molecular organic substances or ions such as copper or other metal impurities were released from

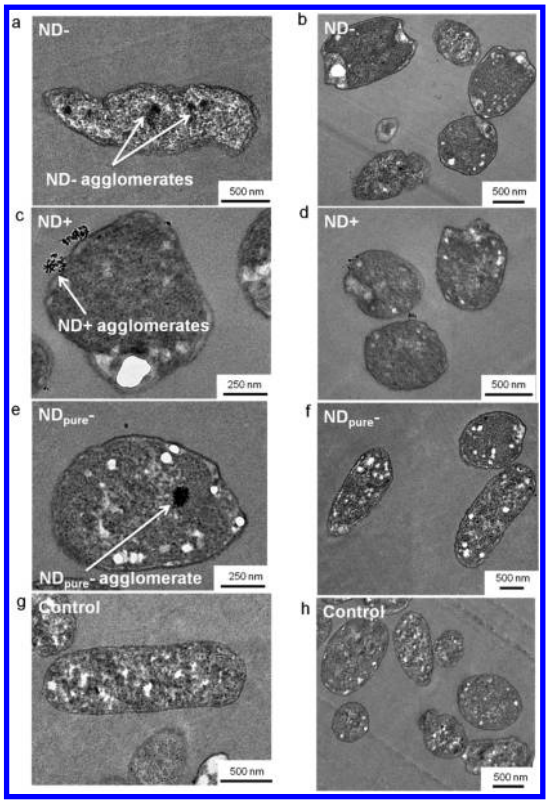


**Figure 4. TEM images indicate that, at sublethal ND concentrations of 0.5 mg/L, ND− is incorporated into *E. coli* cells and seems to deform the cellular shape (a, b). ND+ seems mainly to bind to cellular surface structures (c, d). Similar to ND−, agglomerates of negatively charged $ND_{pure}$− are also found inside the cells, but they do not alter bacterial morphology (e, f), showing similar cell shapes to the ND-free control of *E. coli* (g, h).**

the NDs and are responsible for the compromised bacterial viability. Instead, we conclude that antibacterial properties must be present on the ND surface itself. In fact, an interesting observation was that dialyzed NDs lost their antibacterial properties by consecutive dialysis steps along with a change in the zeta potential of the particles, suggesting that an interaction of NDs with the cellulose dialysis membrane alters surface functionalities, *i.e.*, by the loss of reactive oxygen groups or charges. Our hypothesis was supported by the observation that the value of the zeta potential of ND− decreased after dialysis, leading to a weaker negatively charged surface.

Upon closer inspection of the FTIR data (Figure 2), a comparison of the different surface groups revealed one striking difference for the bactericidal ND types in comparison to the ND types that do not show antibacterial activity. Spectra of the bactericidal ND− and $ND_{raw}$ contained a distinct acid anhydride bond, as indicated by C═O stretches at 1850−1750 $cm^{-1}$, which could not be found for the other ND types (Figure 3). Collectively, all ND species showed characteristic absorption bands for the oxygen-containing functional groups such as hydroxyl groups at 3300−2500 $cm^{-1}$, alkyls derived from $sp^3$-carbon at 3000−2800 $cm^{-1}$, and carboxylic C═O stretches at 1750−1700 $cm^{-1}$. Aromatic C═C at 1600−1400 $cm^{-1}$ were present only for $ND_{raw}$, while the other NDs lost their aromatic bonds after oxidation caused by conversion of $sp^2$- into $sp^3$-hybridized carbon.[22]

The discussed evidence from dialysis and FTIR analysis indicate that the surface chemistry of NDs seems to be the driving force of the observed antibacterial effects. To further test this hypothesis, we designed an experiment based on the coverage and inhibition of functional surface groups. For this, proteins were incubated with NDs prior to bacterial tests. First, we chose fetal bovine serum (FBS), that is used as an additional protein source for most cell culture experiments. Because nearly all publications on the toxicity of ND were performed on eukaryotic cells in FBS-containing cell medium, our bacterial tests in the presence of relevant FBS concentrations also allow a comparison with reported data on ND toxicity. FBS features a broad composition of different proteins containing a total protein content of 38 mg/mL, in which albumin is the most prominent protein featuring a content of around 60%. Interestingly, after the addition of 10% FBS, which is a realistic cell culture concentration, the antibacterial activity of all ND types against *E. coli* and *B. subtilis* disappeared (Figure 5a,b). Only ND− still demonstrated a slight antibacterial effect by reducing bacterial viability by 20−40%. Decreasing FBS concentrations also led to a reduced inhibition of the antibacterial activity of ND. Bovine serum albumin (BSA) was also tested and induced an analogous inhibition corresponding to the amount of BSA that is present in FBS (Supplementary Figure 3). However, BSA concentrations corresponding to the total protein content of FBS were not as potent as FBS in inhibiting the bactericidal properties of NDs. This indicates that additional molecules and substances can also be responsible for the inhibition of the antibacterial activity. In fact, even plain Dulbecco's modified Eagle medium (Life Technologies, Germany), which contains mainly glucose, ions, and amino acids, inhibited the antibacterial potential of NDs (data not shown). Consequently, the addition of proteins or small organic compounds strongly affects the bactericidal properties of NDs and could be used to control the extent of bactericidal action inflicted by NDs.

Generally, all types of NDs exhibit varying degrees of oxygen-containing functional groups such as hydroxyl and carboxyl groups, lactones, ketones, acid anhydrides, and ethers on their surfaces.[23] However, the occurrence and number of any of these groups depends on the ND powder and the pretreatment procedures. Our data suggest a direct correlation between individual oxygen-containing surface groups and the extent of reducing bacterial viability. Similar observations have been made by Chng and Pumera,[24] who showed that surface functionalities of graphene oxide materials differed significantly after four different

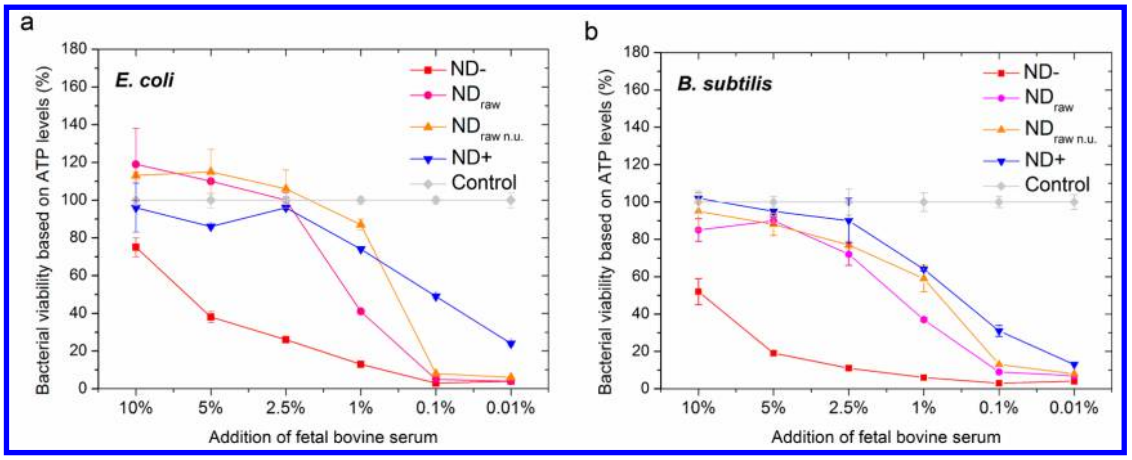


**Figure 5. Fetal bovine serum inhibits the antibacterial properties of NDs. The addition of increasing concentrations of FBS prevents the antibacterial ND types (500 mg/L) from compromising the viability of (a) *E. coli* and (b) *B. subtilis*.**

oxidation pretreatments. As a result, toxicity on A549 human lung cells varied significantly for these four different materials and clearly correlated to the amount of oxygen-containing groups and the types of surface groups.[24]

Regarding our materials, when using the partially oxidized ND powder (grade G01), annealing in air causes further oxidation of surface groups, leading to a prevalence of carboxyl groups, ketones, and lactones. However, in contrast to extrapurified powder (grade G02), the oxidation of the surface groups is incomplete, resulting in residual acid anhydride and carbonyl groups. Carboxylic acid groups in acid anhydride forms are highly reactive toward nucleophilic additions and are prone to various reactions.[25] Our experiments indicate that the reactive groups on ND− and $N_{Draw}$/$ND_{raw\ n.u.}$ disappear when interacting with other functional groups, such as from the cellulose membrane or from proteins in the cell medium. When these reactive groups are removed, the bactericidal properties of the NDs decrease simultaneously. We suggest that these reactive groups can form covalent bonds with adjacent proteins and molecules on cell walls or bind to intracellular components. This coupling inhibits vital enzymes and proteins, leading to a rapid collapse of the bacterial metabolism and finally cell death. In summary, we propose that nonspecific interactions of the highly reactive ND surfaces with biomolecules contribute to the described antibacterial activities.

However, on $ND_{pure}$, all surface moieties are fully oxidized and the only groups that are present on negatively charged $ND_{pure}$ ($ND_{pure}$−) are carboxyl groups, which are not as reactive as acid anhydride groups. $ND_{pure}$− therefore exhibits an isotropic surface with a homogeneous distribution of uniform charges. On the contrary, as discussed in the literature,[26,27] ND− and $ND_{raw}$/$ND_{raw\ n.u.}$ exhibit an anisotropic surface with irregularly distributed functional groups on the different facets of the ND material. This anisotropy might further add to the antibacterial action of ND by denaturing adsorbed proteins.

The origin of the positive charges on ND+ and $ND_{pure}$+ is still a point of debate among the ND research community.[22,28] Although we do not see the characteristic acid anhydride band in our ND+ samples, we assume that the less pronounced antibacterial properties of ND+ might also be caused by reactive oxygen surface groups.

A variety of studies demonstrated the biocompatibility of small detonation NDs on different eukaryotic cells,[29−31] but some hints appeared that susceptibilities are different for various cells, suggesting that ND might be toxic for eukaryotic stem cells[3] and for protozoa,[18] while exhibiting a nontoxic nature for the multicellular eukaryotic organism *Caenorhabditis elegans*.[32] Furthermore, NDs were successfully applied for biomedical applications. As a drug carrier, ND-conjugated chemotherapeutics exhibited a significantly decreased *in vivo* toxicity in a mouse model of liver and mammary cancer compared to standard treatments with doxorubicin,[33] and fluorescent NDs were effective in identifying and tracking transplanted lung stem/progenitor cells *in vivo*.[34]

Regarding bacteria, only a few studies exist at the time of writing. Adhesion behavior of the bacterium *Pseudomonas aeruginosa* was investigated on superhydrophobic nanocrystalline diamond surfaces and compared with silver and copper surfaces. Results for the nanocrystalline surface revealed a more bactericidal and antiadhesive surface than for silver, but not for copper.[16] NDs were used as biolabels and carriers for lysozymes to kill bacterial cells, and lysozyme functionalized NDs were effective in inhibiting bacterial growth, but antibacterial properties of unfunctionalized NDs were not analyzed.[17]

Eukaryotic cells are mostly cultivated in the presence of essential amino acids and proteins. Consequently, we suggest that experimental conditions can significantly influence the resulting toxic effects of NDs.

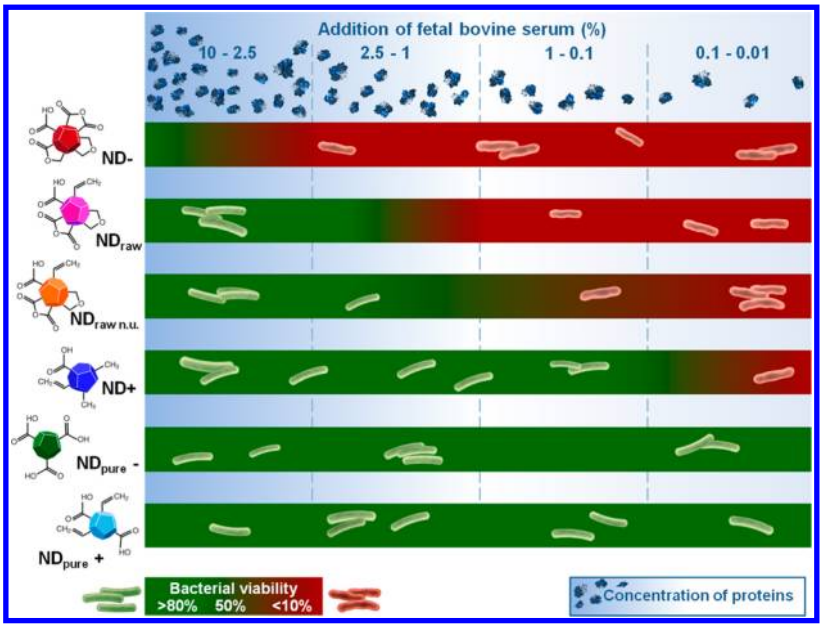


**Figure 6. Antibacterial properties and biocompatibility of the studied NDs. Antibacterial activity of negatively charged partially oxidized NDs can be controlled *via* the protein concentration. While at protein concentrations of around 0.01−0.1% dispersions of 500 mg/L of ND− and $ND_{raw}$/$ND_{raw\ n.u.}$ exhibit extraordinary antibacterial properties against bacteria, protein concentrations of 2.5−10% inhibit the bactericidal properties of these types of NDs.**

The use of proteins and a variety of supplemental ingredients could cause a decrease or even inhibition of the bactericidal potential of NDs by covering reactive oxygen groups. Our findings indicate that increasing concentrations of FBS, BSA, or even ingredients of protein-free cell media decreases the antibacterial properties of the partially oxidized ND types. Using a salt buffer for all bacterial tests, we demonstrated that some ND types exhibit striking antibacterial properties when applied in simple aqueous buffer systems (Figure 6). As widely documented, proteins from biological fluids rapidly cover nanoparticles,[35] and the protein-mediated inhibition of antibacterial properties might limit the scope for intended antimicrobial applications. Simultaneously, the addition of proteins allows the controlled deactivation of the ND surfaces, which might enhance biocompatibility and mitigate safety concerns.

To further classify the antibacterial potential of ND− and $ND_{raw}$/$ND_{raw\ n.u.}$, we compared the effects of NDs on bacterial viability (Figure 3) with that of silver nanoparticles NM300 K with a particle size of around 20 nm,[36] which have a well-known antibacterial potential.[37] At concentrations of 50 mg/L, ND− and $ND_{raw}$/$ND_{raw\ n.u.}$ had the same antibacterial effect as silver nanoparticles (Figure 3a,b and Supplementary Figure 4). Thus, this comparison with bactericidal silver nanoparticles indicates that NDs are very potent candidates for antibacterial applications.

## CONCLUSION

In summary, the data presented demonstrate a strong bactericidal activity of NDs containing partially oxidized surfaces. This activity is most likely based on reactive oxygen-containing surface groups of the bactericidal ND types that foster interactions of these NDs with cellular components, while the anisotropic distribution of charges on the ND surface facilitates alterations in bacterial surfaces. As the bactericidal potential of NDs is inhibited by proteins, the extent and the duration of the antibacterial action of NDs can be modulated by application of proteins. Improvements of the pretreatment procedures for ND production may allow a better control of the surface functionalities of NDs, which could facilitate the generation of tailored antibacterial NDs for specific applications.

## METHODS

**Preparation of ND Suspensions.** Detonation diamond nanopowder was purchased from Plasmachem GmbH, Berlin, Germany, in two different purity grades (G01 and G02 grade). Dispersing of the NDs was carried out according to Hees *et al.*[19] G01 powder without further treatment was dispersed in water featuring a resistivity of >18.2 MΩ $cm^{-1}$ ($ddH_2O$) to obtain a dispersion of $ND_{raw}$ exhibiting an ND concentration of 5000 mg/L ($ND_{raw\ n.u.}$). Additionally, raw ND powder was dispersed in $ddH_2O$ using ultrasonication at 250 W for 3 h ($ND_{raw}$). For the production of negatively charged NDs (ND−), 1 g of the powder (G01 grade) was annealed for 5 h at 450 °C in air. For positively charged NDs (ND+), 1 g of the powder was annealed for 5 h at 500 °C at 1 bar $H_2$ atmosphere. The same procedure was followed for G02 grade powder, resulting in $ND_{pure}$− and $ND_{pure}$+. The pretreated powders were dispersed and ultrasonicated for 3 h in 100 mL of $ddH_2O$. Afterward, the dispersions were centrifuged twice for 1 h at 16000*g* to remove remaining larger aggregates. The resulting

dispersions contained about 5000 mg/L NDs and showed a pH value of 7.

**ND Dialysates.** Five milliliter aliquots of the ND dispersions (5000 mg/L) were dialyzed against 45 mL of $ddH_2O$ to obtain particle-free dialysates that were tested for possible antibacterial effects caused by additives or impurities. Dialysis was performed at RT overnight, and the resulting dialysates correlated to ND dilutions of 1:10.

**ND Characterization.** *Stability and Particle Morphology.* Zeta potential measurements were performed using 5000 mg/L ND dispersions in $ddH_2O$ (pH $\approx$ 7) that were analyzed by a colloidal vibration current probe (DT1200, Quantachrom, Ödelzhausen, Germany). The hydrodynamic diameter and particle size distribution of the ND samples were analyzed by dynamic light scattering using a Beckman-Coulter Delsa Nano C photospectrometer (Beckman Coulter Inc., Brea, CA, USA) at a backscattering angle of 165°. The data were evaluated *via* intensity and number distributions. Sizes and zeta potential for $ND_{raw}$ and $ND_{raw\ n.u.}$ were not measured due to polydispersity.

*Impurity Analysis: Copper and Zinc.* To quantify the amount of the main heavy metal impurities of NDs, ICP-OES analysis of Cu and Zn was performed using an Optima 7300 DV spectrometer, PerkinElmer, and a CETAC Technologies autosampler. For sample preparation, an *aqua regia* digestion of the NDs was performed according to standard procedures.[21]

*Determination of Functional Surface Groups Using FTIR.* FTIR spectroscopy was performed according to standard procedures[38] using KBr pellets. Spectra were measured in transmission mode using an Avatar 370 FTIR spectrometer, Thermo Nicolet.

*Antibacterial Tests. B. subtilis* and *E. coli* were purchased from Deutsche Sammlung Mikroorganismen and Zellkulturen (DSMZ), Braunschweig, Germany. *B. subtilis* (DSMZ No. 1088) and *E. coli* K12 (DSMZ No. 1077) were used as glycerol stocks to inoculate defined overnight cultures. Bacteria were washed once with 25 mM 4-(2-hydroxyethyl)piperazine-1-ethanesulfonic acid buffer (HEPES) (pH 7.2), and the cell pellet collected by centrifugation was resuspended in HEPES to a final cell concentration of approximately $2 \times 10^8$ cells/mL according to McFarland standards.[39]

Bacterial cells were incubated with ND concentrations of 5, 50, and 500 mg/L at 22 °C and 200 rpm for 15 min. For impurity testings, bacterial suspensions were incubated with dialysates correlating with ND dispersions of 50 and 5 mg/L. For controls, $ddH_2O$ was added instead of ND stock dispersions. After incubation, the amount of ATP was determined using a luminescence BacTiterGlo assay (Promega No. G8231, Germany). All experiments were performed as duplicates, and tests were repeated on two independent days to obtain adequate reproducibility ($n = 4$). To exclude an inactivation of the enzymatic ATP assay by NDs, NDs were mixed with ATP and the luminescence of the assay was quantified. Luminescence levels were only slightly altered in the presence of the six ND species investigated, but the influence of NDs on luminescence did not correlate with the observed antibacterial properties of NDs (Supplementary Figure 5).[40] The slight effects of NDs on the assay were compensated by subtracting the deviation of the luminescence of the respective ND types from the results.

Next, colony-forming units were counted by plating bacterial suspensions onto agar plates (aerobic count plate and coliform count plate, 3M, Germany). Appropriate dilutions of bacteria in 25 mM HEPES were prepared and applied to the plates. CFU were determined after incubation at 37 °C for 24–48 h.

The effect of copper impurities was analyzed by incubating *E. coli* with copper(II) sulfate in the concentrations of 3, 15, and 30 $\mu$M, and viability of bacterial cells was analyzed as described above.

The antibacterial effect of NDs was compared with NM300 K silver nanoparticles that were supplied as stock suspensions of 2 g/L. The NM300 K dispersion was produced by RAS Materials (Regensburg, Germany) and provided by Joint Research Center (JRC). Silver nanoparticle concentrations of 0.5, 5, and 50 mg/L were applied, and incubation with bacteria was performed as described above.

To investigate the inhibitory effect of proteins on the antibacterial properties of NDs, different concentrations of FBS (Gibco, Life Technologies, Germany) were added to the ND dispersions (500 mg/L) prior to their use for bacterial tests.

*Uptake of NDs.* To analyze ND uptake by bacteria, after incubation with 0.5 mg/L ND, *E. coli* cells were embedded in agarose, fixed by the standard glutaraldehyde–$OsO_4$ method, and stained with uranyl acetate.[41] Ultrathin sections were analyzed by transmission electron microscopy (EM 900, Zeiss, Germany).

*Conflict of Interest:* The authors declare no competing financial interest.

*Acknowledgment.* M.M. is grateful for funding by the DFG through grant MA4795/5-1.

*Supporting Information Available:* Additional data showing the weak antibacterial effect of copper impurities in the ND dispersions, the viability of *E. coli* after incubation with ND dialysates, the effect of BSA on the antibacterial activity of ND, as well as the antibacterial effect of comparable silver nanoparticle dispersions are supplied. This material is available free of charge *via* the Internet at http://pubs.acs.org.

## REFERENCES AND NOTES


1. Yang, K.; Li, Y. J.; Tan, X. F.; Peng, R.; Liu, Z. Behavior and Toxicity of Graphene and Its Functionalized Derivatives in Biological Systems. *Small* **2013**, *9*, 1492–1503.
2. Kang, S.; Herzberg, M.; Rodrigues, D. F.; Elimelech, M. Antibacterial Effects of Carbon Nanotubes: Size Does Matter. *Langmuir* **2008**, *24*, 6409–6413.
3. Xing, Y.; Xiong, W.; Zhu, L.; Osawa, E.; Hussin, S.; Dai, L. M. DNA Damage in Embryonic Stem Cells Caused by Nanodiamonds. *ACS Nano* **2011**, *5*, 2376–2384.
4. Singh, N.; Manshian, B.; Jenkins, G. J. S.; Griffiths, S. M.; Williams, P. M.; Maffeis, T. G. G.; Wright, C. J.; Doak, S. H. Nanogenotoxicology: The DNA Damaging Potential of Engineered Nanomaterials. *Biomaterials* **2009**, *30*, 3891–3914.
5. Nel, A. E.; Madler, L.; Velegol, D.; Xia, T.; Hoek, E. M. V.; Somasundaran, P.; Klaessig, F.; Castranova, V.; Thompson, M. Understanding Biophysicochemical Interactions at the Nano-Bio Interface. *Nat. Mater.* **2009**, *8*, 543–557.
6. Krueger, A.; Kataoka, F.; Ozawa, M.; Fujino, T.; Suzuki, Y.; Aleksenskii, A. E.; Vul', A. Y.; Ōsawa, E. Unusually Tight Aggregation in Detonation Nanodiamond: Identification and Disintegration. *Carbon* **2005**, *43*, 1722–1730.
7. Schrand, A. M.; Hens, S. A. C.; Shenderova, O. A. Nanodiamond Particles: Properties and Perspectives for Bioapplications. *Crit. Rev. Solid State* **2009**, *34*, 18–74.
8. Roy, S.; Mitra, K.; Desai, C.; Petrova, R.; Mitra, S. Detonation Nanodiamonds and Carbon Nanotubes as Reinforcements in Epoxy Composites—a Comparative Study. *J. Nanotechnol. Eng. Med.* **2013**, *4*, 011008.
9. Guo, Y.; Li, S.; Li, W.; Moosa, B.; Khashab, N. M. The Hofmeister Effect on Nanodiamonds: How Addition of Ions Provides Superior Drug Loading Platforms. *Biomater. Sci.* **2014**, *2*, 84–88.
10. Chang, Y. R.; Lee, H. Y.; Chen, K.; Chang, C. C.; Tsai, D. S.; Fu, C. C.; Lim, T. S.; Tzeng, Y. K.; Fang, C. Y.; Han, C. C.; *et al.* Mass Production and Dynamic Imaging of Fluorescent Nanodiamonds. *Nat. Nanotechnol.* **2008**, *3*, 284–288.
11. Vlasov, I. I.; Shiryaev, A. A.; Rendler, T.; Steinert, S.; Lee, S.-Y.; Antonov, D.; Voros, M.; Jelezko, F.; Fisenko, A. V.; Semjonova, L. F.; *et al.* Molecular-Sized Fluorescent Nanodiamonds. *Nat. Nanotechnol.* **2014**, *9*, 54–58.
12. Krueger, A. The Structure and Reactivity of Nanoscale Diamond. *J. Mater. Chem.* **2008**, *18*, 1485–1492.
13. Zhang, Q.; Mochalin, V. N.; Neitzel, I.; Knoke, I. Y.; Han, J.; Klug, C. A.; Zhou, J. G.; Lelkes, P. I.; Gogotsi, Y. Fluorescent Plla-Nanodiamond Composites for Bone Tissue Engineering. *Biomaterials* **2011**, *32*, 87–94.
14. Mochalin, V. N.; Shenderova, O.; Ho, D.; Gogotsi, Y. The Properties and Applications of Nanodiamonds. *Nat. Nanotechnol.* **2012**, *7*, 11–23.

15. Xing, Y.; Dai, L. M. Nanodiamonds for Nanomedicine. *Nanomedicine* **2009**, *4*, 207–218.
16. Medina, O.; Nocua, J.; Mendoza, F.; Gomez-Moreno, R.; Avalos, J.; Rodriguez, C.; Morell, G. Bactericide and Bacterial Anti-Adhesive Properties of the Nanocrystalline Diamond Surface. *Diam. Relat. Mater.* **2012**, *22*, 77–81.
17. Perevedentseva, E.; Cheng, C. Y.; Chung, P. H.; Tu, J. S.; Hsieh, Y. H.; Cheng, C. L. The Interaction of the Protein Lysozyme with Bacteria E-Coli Observed Using Nanodiamond Labelling. *Nanotechnology* **2007**, *18*, 1–7.
18. Lin, Y. C.; Perevedentseva, E.; Tsai, L. W.; Wu, K. T.; Cheng, C. L. Nanodiamond for Intracellular Imaging in the Microorganisms in Vivo. *J. Biophotonics* **2012**, *5*, 838–847.
19. Hees, J.; Kriele, A.; Williams, O. A. Electrostatic Self-Assembly of Diamond Nanoparticles. *Chem. Phys. Lett.* **2011**, *509*, 12–15.
20. Silhavy, T. J.; Kahne, D.; Walker, S. *The Bacterial Cell Envelope*; Cold Spring Harbor Laboratory Press: New York, 2010; Vol. 2.
21. Baumann, J.; Sakka, Y.; Bertrand, C.; Köser, J.; Filser, J. Adaptation of the Daphnia Sp. Acute Toxicity Test: Miniaturization and Prolongation for the Testing of Nanomaterials. *Environ. Sci. Pollut. Res.* **2013**, *21*, 2201–2213.
22. Osswald, S.; Yushin, G.; Mochalin, V.; Kucheyev, S. O.; Gogotsi, Y. Control of sp(2)/sp(3) Carbon Ratio and Surface Chemistry of Nanodiamond Powders by Selective Oxidation in Air. *J. Am. Chem. Soc.* **2006**, *128*, 11635–11642.
23. Desai, C.; Chen, K.; Mitra, S. Aggregation Behavior of Nanodiamonds and Their Functionalized Analogs in an Aqueous Environment. *Env. Sci. Process. Impact* **2013**, *16*, 518–523.
24. Chng, E. L. K.; Pumera, M. The Toxicity of Graphene Oxides: Dependence on the Oxidative Methods Used. *Chem.—Eur. J.* **2013**, *19*, 8227–8235.
25. Cloete, W. J.; Verwey, L.; Klumperman, B. Permanently Antimicrobial Waterborne Coatings Based on the Dual Role of Modified Poly(Styrene-co-Maleic Anhydride). *Eur. Polym. J.* **2013**, *49*, 1080–1088.
26. Barnard, A. S.; Osawa, E. The Impact of Structural Polydispersivity on the Surface Electrostatic Potential of Nanodiamond. *Nanoscale* **2014**, *6*, 1188–1194.
27. Barnard, A. S.; Sternberg, M. Crystallinity and Surface Electrostatics of Diamond Nanocrystals. *J. Mater. Chem.* **2007**, *17*, 4811–4819.
28. Williams, O. A.; Hees, J.; Dieker, C.; Jager, W.; Kirste, L.; Nebel, C. E. Size-Dependent Reactivity of Diamond Nanoparticles. *ACS Nano* **2010**, *4*, 4824–4830.
29. Schrand, A. M.; Huang, H.; Carlson, C.; Schlager, J. J.; Ōsawa, E.; Hussain, S. M.; Dai, L. Are Diamond Nanoparticles Cytotoxic?. *J. Phys. Chem. B* **2006**, *111*, 2–7.
30. Zhang, X. Y.; Wang, S. Q.; Liu, M. Y.; Hui, J. F.; Yang, B.; Tao, L.; Wei, Y. Surfactant-Dispersed Nanodiamond: Biocompatibility Evaluation and Drug Delivery Applications. *Toxicol. Res.-UK* **2013**, *2*, 335–342.
31. Karpukhin, A. V.; Avkhacheva, N. V.; Yakovlev, R. Y.; Kulakova, I. I.; Yashin, V. A.; Lisichkin, G. V.; Safronova, V. G. Effect of Detonation Nanodiamonds on Phagocyte Activity. *Cell Biol. Int.* **2011**, *35*, 727–733.
32. Mohan, N.; Chen, C.-S.; Hsieh, H.-H.; Wu, Y.-C.; Chang, H.-C. In Vivo Imaging and Toxicity Assessments of Fluorescent Nanodiamonds in Caenorhabditis Elegans. *Nano Lett.* **2010**, *10*, 3692–3699.
33. Chow, E. K.; Zhang, X. Q.; Chen, M.; Lam, R.; Robinson, E.; Huang, H. J.; Schaffer, D.; Osawa, E.; Goga, A.; Ho, D. Nanodiamond Therapeutic Delivery Agents Mediate Enhanced Chemoresistant Tumor Treatment. *Sci. Transl. Med.* **2011**, *3*, 73ra21.
34. Wu, T. J.; Tzeng, Y. K.; Chang, W. W.; Cheng, C. A.; Kuo, Y.; Chien, C. H.; Chang, H. C.; Yu, J. Tracking the Engraftment and Regenerative Capabilities of Transplanted Lung Stem Cells Using Fluorescent Nanodiamonds. *Nat. Nanotechnol.* **2013**, *8*, 682–689.
35. Monopoli, M. P.; Aberg, C.; Salvati, A.; Dawson, K. A. Biomolecular Coronas Provide the Biological Identity of Nanosized Materials. *Nat. Nanotechnol.* **2012**, *7*, 779–786.
36. Matzke, M.; Jurkschat, K.; Backhaus, T. Toxicity of Differently Sized and Coated Silver Nanoparticles to the Bacterium Pseudomonas Putida. *Ecotoxicology* [online early access]. DOI: 10.1007/s10646-014-1222-x.. Published online: Mar 22, 2014. http://www.ncbi.nlm.nih.gov/pubmed/24659347 (accessed May 26, 2014).
37. Chernousova, S.; Epple, M. Silver as Antibacterial Agent: Ion, Nanoparticle, and Metal. *Angew. Chem., Int. Ed.* **2013**, *52*, 1636–1653.
38. Chen, Z.-H.; Zhao, Y.; Wang, P.; Chen, S.-S.; Sun, W.-Y. Zinc(II) and Cadmium(II) Complexes with Mixed 1,3-Di-(1H-Imidazol-4-yl)Benzene and Cyclohexanedicarboxylate Ligands: Synthesis, Structure and Property. *Polyhedron* **2014**, *67*, 253–263.
39. McFarland, J. The Nephelometer - an Instrument for Estimating the Number of Bacteria in Suspensions Used for Calculating the Opsonic Index and for Vaccines. *J. Am. Med. Assoc.* **1907**, *49*, 1176–1178.
40. Puzyr, A. P.; Pozdnyakova, I. O.; Bondar, V. S. Design of a Luminescent Biochip with Nanodiamonds and Bacterial Luciferase. *Phys. Solid State* **2004**, *46*, 761–763.
41. Puzyr, A. P.; Baron, A. V.; Purtov, K. V.; Bortnikov, E. V.; Skobelev, N. N.; Moginaya, O. A.; Bondar, V. S. Nanodiamonds with Novel Properties: A Biological Study. *Diam. Relat. Mater.* **2007**, *16*, 2124–2128.